



**Abstract:** Flood is one of the most disastrous disasters in the world inflicting massive economic losses and deaths on human society, and it is particularly true for China which is the home to the largest population in the world. However, no comprehensive and thorough investigations have been done so far addressing spatiotemporal properties and relevant driving factors of flood disasters in China. Here we investigated changes of



23 flood disasters in both space and time and their driving factors behind using statistical  
24 data of the meteorological disasters from Statistical Yearbooks and also hourly rainfall  
25 data at 2420 stations covering a period of 1984-2007. GeoDetector method was used to  
26 analyze potential driving factors behind flood disasters. We found no consistent  
27 extreme rainfall trend across China with exceptions of some sporadic areas. However,  
28 recent years witnessed increased frequency of rainstorm-induced flood disasters within  
29 China and significant increase in the frequency of flood disasters in the Yangtze River,  
30 Pearl River and Southeastern coasts. Meanwhile, reduced flood-related death rates in  
31 the regions with increased flood frequency indicated enhanced flood-mitigation  
32 infrastructure and facilities. However, increased flood-induced affected rates and direct  
33 economic losses per capita were found in the northwestern China. In addition,  
34 contributions of influencing factors to the spatio-temporal distribution of flood disasters  
35 analyzed by GeoDetector are shifting from one region to another. While we found that  
36 rainfall changes play the overwhelming role in driving occurrences of flood disasters,  
37 other factors also have considerable impacts on flood disasters and flood disaster-  
38 induced losses such as topographical features and spatial patterns of socio-economy.  
39 Wherein, topography acts as the key factor behind the characteristics of spatial  
40 distribution of flood disasters in China.

41 **Key words:** Rainstorm-induced flood disasters; Heavy rainfall; Driving factors;  
42 GeoDetector

43

## 44 1. Introduction

45 China is the largest country in terms of population and is amongst the most flood-prone  
46 countries worldwide, inflicting an average of 4327 deaths per year since 1950, and 20-  
47 billion-dollar direct economic losses per year during 1990-2017 (Ye et al., 2018). Due



48 to its special geographical location and massive impacts from the East Asian monsoon,  
49 the floods caused by heavy rains are particularly serious and strong in some regions of  
50 China (Chen and Sun, 2015). The past 50 years and in particular since 1990s China  
51 witnessed significantly enhanced frequency and intensity of extreme weather events  
52 due to warming climate (Zhang et al., 2013), thus severe floods occurred more often  
53 than before (Shi et al., 2004). Besides, rapid urbanization over China in recent years  
54 triggers spatial gathering of population and wealth over the flood plains and hence  
55 aggravated flood risk can be well expected (Li et al., 2016b; Du et al., 2018). The  
56 complex combinations of changes in hydro-meteorological extremes and increasing  
57 impacts of human activities can have paramount effects on the frequency and magnitude  
58 of flood disasters (Zhang et al., 2015b). Therefore, it is of great importance to  
59 comprehensively understand the temporal and spatial changes of flood disasters and the  
60 influencing factors behind under the context of the global warming, which provides  
61 countermeasures to flood risk management and reduces loss of life and property.

62 Global warming as a result of human-induced emission of greenhouse gases is  
63 accelerating the global hydrological cycle (Arnell, 1999; Allen and Ingram, 2002;  
64 Zhang et al., 2013). Meanwhile, the accelerated hydrological process is altering the  
65 spatial-temporal patterns of rainfall which can trigger increased occurrences of rainfall  
66 extremes (Easterling et al., 2000) and in turn increased occurrences of floods and  
67 droughts in many regions of the world (Easterling et al., 2000; Hu et al., 2018). Willner  
68 et al. (2018) indicated that changes in the hydrological cycle can cause a strong  
69 increase in globally aggregated direct losses due to fluvial floods. Besides, large  
70 direct losses were observed in China, the United States, Canada, India, Pakistan and  
71 various countries of the European Union (Willner et al., 2018), which implies that, with



72 the current regional river protection level or without further adaptation efforts, large  
73 parts of densely populated areas will experience more floods in the future due to an  
74 increase in rainfall extremes (Willner et al., 2018). These findings also evidenced  
75 critical relations between rainfall extremes and flood risks over the globe. Hirabayashi  
76 et al. (2013) indicated that, in certain areas of the world, flood frequency is projected  
77 to decrease. Van Vuuren et al. (2011) indicated that the global exposure to floods would  
78 increase depending on the degree of warming, but inter-annual variability of the  
79 exposure may imply the necessity of adaptation before significant warming. Therefore,  
80 massively increasing human concerns have been attached to floods and relevant losses  
81 of human life, society property and also socio-economy (Van Vuuren et al., 2011;  
82 Willner et al., 2018). In this case, flood means much for human society and it is  
83 particularly the case for China, a country with the largest population and fast economic  
84 growth rate. This point constitutes the significance of this study.

85 Numerous studies have been done addressing changes of flood disasters over  
86 China. Some studies focused on the temporal and spatial changes of flood disasters  
87 based on meteorological and hydrological datasets and also historical statistical data  
88 (Zhang et al., 2015a; Zhang et al., 2018b) and impacts on social economy in provincial  
89 administrative units at national scales (Huang et al., 2012). Besides, previous studies  
90 analyzed the flood disasters from the perspective of the trends of frequency, intensity  
91 and other characteristics of extreme rainfall events (Jiang et al., 2007; Zhang et al., 2008;  
92 Lu and Fu, 2010; Zhang et al., 2015a). While, some studies focused on flood disaster  
93 risk assessment at watershed or national levels (Li et al., 2016a). However, few studies  
94 were reported addressing flood disasters at county scales in China. Wang et al. (2008)  
95 firstly investigated the spatiotemporal patterns of flood and drought disasters in county-





96 level administrative units across China using data collected from newspapers, which  
97 provided a scientific basis for flood risk identification. Li et al. (2018) firstly adopted  
98 county-level meteorological disaster census database reported by meteorological  
99 departments across China, combined with daily rainfall observations from national  
100 meteorological stations to analyze the relationship between extreme rainfall and  
101 impacts of flood disasters, no evident relationships were found between high-value  
102 areas of heavy rain and regions of severe flood disasters. It should be clarified that flood  
103 disaster is a highly complex system involving flood hazard, disaster formative  
104 environment and exposure (Shi, 2002). Thus, a variety of environmental and human-  
105 related factors need to be included for further investigation of this subject and to better  
106 understand the mechanism behind flood disasters. This is the major motivation behind  
107 this current study.

108 In this study, spatiotemporal variations of flood disasters across China were  
109 analyzed. The major objectives of this study are to: (1) differentiate extreme rainfall  
110 changes and flood disasters at county-level across China based on statistical records  
111 from Statistical Yearbooks and also in situ observed rainfall; (2) to quantify fractional  
112 contribution of different influencing factors such as land use and land cover change and  
113 socio-economic characteristics to floods; and (3) to deepen human understanding of the  
114 mechanism behind the occurrence of flood disasters. What's more, we should  
115 emphasize the significance of this current study in global sense that China is the largest  
116 country in population with about 70% of population along the coastal regions (Zhang  
117 et al., 2017) and with massive exposure to natural disasters such as floods in this current  
118 study. In this sense, this current study provides a pretty typical case study for global  
119 human mitigation to floods disasters. Therefore, hydrometeorological extremes in  
120 China have been arousing increasing international concerns (Zhang et al., 2013, 2016,



2017, 2018b). Besides, China is located in the East Asia, eastern part of the largest Eurasia continent, and western edge of the largest Pacific Ocean. Furthermore, booming urbanization, fast development of water infrastructures, intensifying land use and land changes and so on, result in considerably complicated driving factors behind floods. Hence, it is of great scientific significance to develop human knowledge in flooding behaviors in a backdrop of complicated changing environment. Moreover, it is acknowledged to understand flooding behaviors from a global perspective. However, the first step is to obtain detailed information of flooding changes at regional scale. It is always useful and helpful to understand flooding behaviors at global scale based on deep understanding of flooding changes at regional scale. In this sense, this current study is theoretically and scientifically significant in development of human knowledge of flood disasters in a changing environment at regional and global scales.

133

## 134 **2. Data**

The datasets analyzed in this study included the national county-level meteorological disaster census database collected from the historical meteorological disaster dataset of the National Climate Center and Yearbook of Meteorological Disasters in China (<http://data.cma.cn/data/cdcindex/cid/8e65c709b3220e70.html>). The definition of flood disaster in this dataset was in accordance with Wen and Ding (2008). This dataset involves 96 indicators describing each individual severe weather-related disaster events based on the county-level administrative units from 1980-2008 with daily temporal resolution. Besides, this database includes 16 items describing the severe weather events, i.e. occurrence timing, locations, impact on society, agriculture, water resources, industry and traffic facilities as well. This database includes the data by the Ministry of Civil Affairs and the quality was firmly controlled before its release.



146 Based on data integrity and the continuity of time series, the flood-affected population,  
147 the flood-induced deaths and the direct economic loss during 1984 to 2007 were  
148 analyzed in this study. Besides, we sorted out and verified each flood disaster events to  
149 keep rigorousness of the dataset. Moreover, we also screened out rainstorm-induced  
150 floods that have greater impacts on human society. Specifically, the entry criteria for  
151 rainstorm-induced floods are referred to the access standards from the international  
152 disaster databases and relevant literatures (Guha-Sapir et al., 2017). The entry criteria  
153 are set as follows: (1) Deaths: 1 death or more deaths; (2) Flood-affected population:  
154 100 or more people are affected by floods. (3) Damaged cropland: 66700 or more  
155 hectares of croplands were affected by floods (the major economic loss is caused by  
156 flood disaster events over the threshold of 66700 hectares, which is analyzed by Li and  
157 Xu (1995)). (4) Damaged reservoirs: 1 or more water reservoirs were damaged.

158 The hourly rainfall data were obtained from 2420 in situ observatory stations  
159 (<http://data.cma.cn/>). The quality of the hourly rainfall data was firmly controlled  
160 before its release (Zhang et al., 2018a). In addition, we also analyzed the total  
161 population, non-agricultural population, Gross Domestic Product (GDP), elevation and  
162 river system data for attribution analysis (shown in Fig. 1). The population data were  
163 collected from the national demographic yearbook, and the GDP data from China's  
164 county (city) socio-economic statistical yearbook. Moreover, we also used the Digital  
165 Elevation Model (DEM) obtained from the US National Atmospheric and Oceanic  
166 Administration (GLOBE Task Team et al., 1999) and also the river system data  
167 collected from the National Catalogue Service For Geographic Information  
168 (<http://www.webmap.cn/commres.do?method=result100W>).

169

### 170 3. Methods



### 171 3.1 Definition of separated rainfall events

172 In this study, separated rainfall events were defined using the conceptual and  
 173 statistical method proposed by Gaal et al. (2014): The autocorrelation method was used  
 174 to differentiate the rainless intervals by the Pearson correlation coefficient of the hourly  
 175 rainfall series. When the autocorrelation coefficient dropped below a predefined  
 176 significance level, i.e. 5% in this study, the time lag was taken as the waiting time  
 177 between separated rainfall events. Fig. 2 illustrates the autocorrelograms of hourly  
 178 rainfall series at three stations. It can be seen from Fig. 2 that the lag time is about 10  
 179 hours when the autocorrelation coefficient drops below the 5% significance level, so  
 180 10 hours were taken as the waiting time between individual rainfall events.

181 Stations with missing data of  $> 1\%$  of the total rainfall data were excluded from the  
 182 analysis. Therefore, hourly rainfall data at 1876 stations were analyzed in this study.  
 183 The missing data were processed based on the procedure by Zhang et al. (2018a).  
 184 Rainfall values of  $< 0.1$  mm/h were replaced with zero (Gaal et al., 2014). The spatial  
 185 patterns of stations included into/excluded from the analysis of this study were  
 186 illustrated in Fig. 3. In Northern China, hourly rainfall can be observed during flooding  
 187 season only. Therefore, the rainfall decadal variability during flooding season were  
 188 analyzed.

189

### 190 3.2 Detection of trends in rainfall extremes and Kernel density estimation technique

191 The Modified Mann-Kendall (MMK) trend test method (Daufresne et al., 2009)  
 192 was used to evaluate trends in rainfall extremes in this study. Besides, Kernel density  
 193 estimation (KDE) method was used to quantify the occurrence rate of the historical  
 194 flood disaster events. The KDE was used to evaluate the density function of random  
 195 variables following unknown distribution and to figure out the distribution



characteristics of the time series considered in this study. This method has been widely used in distribution evaluations due to the fact that this method does not need assumption of probability distributions (Mudelsee et al., 2003; Zhang et al., 2018b). Below is the estimation of occurrence rates:

$$\lambda(t) = h^{-1} \sum_{i=1}^m K\left(\frac{t-T_i}{h}\right) \quad (1)$$

where  $T_i$  denotes the occurrence timing of the  $i^{\text{th}}$  flood event;  $m$  denotes the total number of events;  $K(\cdot)$  denotes the Kernel function in this study, the Gaussian kernel function was applied (Mudelsee et al., 2003);  $h$  denotes the band width. The optimal window width was determined by the unbiased cross-validation test (Cowling et al., 1996);  $\lambda(t)$  indicates the number of extreme events exceeding threshold given a certain time interval,  $t$ .

### 3.3 The GeoDetector for attribution analysis

In this study, the GeoDetector method was used to investigate influencing factors behind flood disasters. The GeoDetector is a set of statistical methods that detect the spatial variations of a variable and relevant driving forces behind (Wang and Hu, 2012; Li et al., 2013; Onozuka and Hagihara, 2017). This method follows the assumption that given an independent variable,  $Y$ , that has an important influence on a dependent variable  $X$ , the spatial distribution of  $Y$  and  $X$  should concur and hence allows for spatial similarity. The degree of the association between  $X$  and  $Y$  could be measured by  $q$  statistics:

$$q = 1 - \frac{1}{N\sigma^2} \sum_{h=1}^L N_h \sigma_h^2 \quad (2)$$

where  $N$  denotes the number of units of  $Y$  in the study area;  $\sigma^2$  denotes the variance of  $Y$ ;  $L$  denotes the  $L$  strata subdivided by the variable  $X$  ( $h = 1, 2, \dots, L$ ). Different



discretization schemes can modulate the  $q$  values to some extent. Thus the optimal discretization method that has the highest  $q$  value was accepted based on the procedure by Cao et al. (2013).  $N_h$  denotes the number of units of  $Y$  in the stratum  $h$ ;  $\sigma_h^2$  denotes the variance of  $Y$  in the stratum  $h$ . The value of  $q \in [0, 1]$ . The higher  $q$  means the higher association between  $Y$  and  $X$ . In this study,  $Y$  denotes the indexes (flood-induced deaths, flood-affected people and flood-induced economic losses) of flood disasters, and  $X$  denotes the influencing factors as discussed in the Discussion section. Detailed introduction of the algorithms and relevant software scripts can be found at <http://www.geodetector.org/>.

229

## 230 4. Results

### 231 4.1 Trends in the annual maximum rainfall

Trends of annual maximum rainfall (AMR, the largest one-day precipitation amount during one year) were evaluated (Fig. 4). It can be observed from Fig. 4a that stations with different trends of AMR distributed in an exchangeable way. However, relatively discernable spatial pattern of stations with increasing and/or decreasing AMR can still be observed. Increased AMR was observed mainly in southeastern and central-eastern China, or specifically in the middle Pearl River basin, southeastern parts of the Yangtze River basin, the Huai River basin and the lower Yellow River basin. The AMR at 914 out of 1876 stations was in increasing tendency and significant increasing trends can be observed at 102 out of 1876 stations (Fig. 4a). Decreased AMR can be found mainly in the lower and upper Yangtze River basin, the upper Pearl River basin and Hai River basin. Besides, the northeastern China was dominated by decreased AMR. Significantly decreased AMR can be detected at 70 out of 1876 stations across China, and 790 out of 1876 stations were dominated by insignificant decreasing tendency of AMR. In this



245 sense, the amount of the AMR was in moderate changes. Spatial pattern of the trends  
246 in the rainfall duration (Fig. 4b) follows the similar spatial pattern of the trends in the  
247 amount of AMR. However, few stations were dominated by significant decreasing  
248 (65)/increasing (69) rainfall duration. In this sense, rainfall duration was also subject to  
249 no significant trends across China. When it comes to spatial pattern of trends in rainfall  
250 duration, lengthening rainfall duration was found mainly in southern China and in the  
251 lower Yellow River basin, and in the Huai River basin as well. Shortening rainfall  
252 duration was observed mainly in the lower Yangtze River basin and northeastern China.  
253 Fig. 4c shows distinctly different spatial pattern of the trends in the rainfall intensity  
254 when compared to that of the AMR and rainfall durations (Figs. 4a, 4b). No confirmable  
255 and discernable spatial pattern can be identified for rainfall intensity of the AMR (Fig.  
256 4c, the rainfall intensity of the maximum rainfall event per year). Stations with  
257 increasing rainfall intensity distributed amidst those with decreasing rainfall intensity  
258 in an even and exchangeable way. Statistically, significantly increased rainfall intensity  
259 was observed at 93 out of 1876 stations and 47 out of 1876 stations were dominated by  
260 decreased rainfall intensity. Increased rainfall intensity can be identified at 971 stations  
261 and decreased rainfall intensity can be observed at 765 stations.

262 The spatial and temporal evolutions of the rainstorm indexes were analyzed (Fig.  
263 5). The rainstorm event was defined by the rainfall event with rainfall amount of  $> 16$   
264 mm/h in this study. We used a range of spatial interpolation methods in spatial  
265 interpolation analysis in this study and we found similar spatial patterns (figures now  
266 shown here). Besides, the Inverse Distance Weighted (IDW) interpolation method was  
267 widely used and spatial patterns by IDW are similar to the actual situation. Therefore,  
268 we accepted the IDW method in spatial interpolation analysis. It can be seen from Fig.  
269 5 that less rainstorm amount was found mainly in the northwestern, northern and



northeastern China. Besides, most parts of the Tibet Plateau was also dominated by less  
rainstorm amount, e.g.  $< 450$  mm and even  $< 150$  mm. However, larger rainstorm  
amount was observed mainly in the central and southeastern China and parts of the  
eastern China. Left panel graphs indicated expanding regions with smaller rainfall  
amount from 1980s to 2000s, and it is particularly the case in the northeastern China.  
While, shrunk regions with less rainstorm amount were found in northwestern China  
during 1991-2000. Meanwhile, regions with larger rainstorm amount during 1991-2000  
were found mainly in the middle and lower Yangtze River basin and also in the Pearl  
River basin. However, regions with larger rainstorm amount during 2001-2007 were  
found mainly in the Pearl River basin. These results may imply amplification of  
droughts across China over the time with higher drought risks. Similar spatial and  
temporal evolution pattern of rainstorm duration was found (right column of Fig. 5).  
Regions with shorter rainstorm duration expanded during last decades and it is  
particularly true in recent decade. What's more, larger area of regions with longer  
rainstorm duration shrunk in recent years. Significant and widespread shrinking regions  
with longer rainstorm duration imply higher probability of intense precipitation  
processes and hence higher probability of floods and/or flood disasters.

#### 4.2 Spatiotemporal variations of flood frequency

The occurrence rates of flood events were evaluated in seven sub-regions of China  
subdivided based on their geographical divisions (Fig. 6). Increased flood frequency  
can be observed during 1984-2007, the study period considered in this study. Generally,  
similar temporal patterns of flood frequency can be found in Northeastern China,  
Eastern China, Northern China and Central China, i.e. three time intervals with higher  
flood frequency and two time intervals with relatively lower flood frequency can be  
identified. Time intervals with relatively higher flood frequency are respectively 1984-





1990, 1991-2000 and 2001-2007. Two time intervals with relatively lower flood frequency are respectively 1992-1994 and 2000-2003. However, Except for the continuous increasing tendency in the Northwest and Southwest China, there was a decreasing trend during a period of 2000-2003. Larger fluctuations can be found in flood frequency changes in Northeastern, Eastern, Northern and Central China. While, relatively smaller fluctuations in flood frequency changes can be observed in Southern, Northwestern and Southwestern China. Particularly, the Southwestern China is dominated by persistently increasing flood frequency with moderate fluctuations. While, sharp increase and abrupt decrease of flood frequency can be observed at two ends of the flood series (Fig. 6), which can be attributed to boundary effects of the flood series since that fewer data are available at two ends of the time series with larger uncertainty.

Three time intervals with higher flood frequency were analyzed to calculate the annual average frequency, mortality (per million people), the flood-affected rate (%) and the economic loss per capita (unit: RMB converted into 2007 price) (Figs. 7, 8). It can be seen from Fig. 7 that Three time intervals with higher flood frequency were analyzed to calculate the annual average frequency, mortality (per million people), the flood-affected rate (%) and the economic loss per capita (unit: RMB converted into 2007 price) (Figs. 7, 8). It can be seen from Fig. 7 that higher flood frequency can be observed in the Yangtze River basin, the Yellow River basin and also in the Pearl River basin. Besides, larger flood frequency can also be detected in the northeastern China. While, higher flood frequency during 1991-2000 was significantly higher than that during 1984-1990. Increased flood frequency during 1991-2000 when compared to that during 1984-1990 was detected mainly in the middle and lower Yangtze River basin and also the Pearl River basin. Comparatively, reduced flood frequency can be found



320 in northern and northeastern China during 1991-2000 when compared to that during  
321 1984-1990. Besides, more regions with larger flood frequency were found during 1991-  
322 2000 than that during 1984-1990. The time interval of 2001-2007 was characterized by  
323 even higher flood frequency when compared to that during other two time intervals, i.e.  
324 1984-1990 and 1991-2000. Specifically, high flood frequency can be found in the  
325 southwestern China, southern China, southeastern China and also almost entire Yangtze  
326 River basin. Particularly, higher flood frequency can also be observed in some counties  
327 in northwestern China.

328 Decadal changes in the annual number of deaths due to floods per year (Fig. 7)  
329 indicated sporadic distribution of flood-induced mortalities across China. Higher  
330 mortalities can be found in central and southern China. It is surprising to find that some  
331 counties in the northwestern China were also dominated by higher flood-induced losses  
332 (Zhang et al., 2016). Zhang et al. (2012) indicated that, after 1980, the Xinjiang region  
333 in northwestern China is exhibiting a wetting tendency, and the heavy precipitation  
334 extremes tend to occur more severely and frequently. However, the spatial pattern of  
335 the flood-induced mortalities (Fig. 7) are different from that of the flood frequency.  
336 Less counties were characterized by high mortalities during 1991-2000 when compared  
337 to that during 1984-1990. Specifically, sharp decreased flood-induced mortalities can  
338 be found in the middle and the lower Yangtze River and also in the Pearl River basin.  
339 Besides, significant decrease of flood-induced mortalities can also be found in  
340 northeastern China. It is easy to understand that the eastern and central China is highly  
341 economically developed with booming development of socio-economy, and enhanced  
342 human mitigation to floods by construction of levees and flood-mitigated infrastructure  
343 (Ye et al., 2018). However, the mortality rate of some counties in the northwestern  
344 China and northern China such as Xinjiang and Inner Mongolia was in increasing trends.



345 This finding can be attributed to increased rainfall and fast melting snow and ice due to  
346 warming climate (Wen and Song, 2006; Zhang et al., 2016)(...). Besides, lower  
347 development of socio-economy in these regions also make these regions susceptible to  
348 flood disasters.

349 Fig. 8 illustrated spatiotemporal evolutions of the flood-affected rate (ratio of the  
350 annual average flood-affected people in the study period to the total population in each  
351 county) and the direct economic loss per capita in the eastern and central parts of China.  
352 It can be easily observed from Fig. 8 that the flood-affected rate and the direct economic  
353 loss per capita are both increasing during the entire study period in both space and time  
354 (Fig. 8). The Yangtze River basin was in the dominant position in the flood-affected  
355 rate and the direct economic loss per capita. In addition, the flood-affected rate and the  
356 direct economic loss per capita are also in evident increase in the Pearl River basin. It  
357 should be noted here that the northwestern China and parts of the Tibet Plateau are also  
358 dominated by increased flood-affected rate and the direct economic loss per capita.  
359 Besides, difference was still identified in spatial pattern for the flood-affected rate and  
360 the direct economic loss per capita. Larger increase of the direct economic loss per  
361 capita than the flood-affected rate can be found in central, eastern, southern and  
362 northeastern China. Particularly, widespread and larger magnitude of increase in the  
363 direct economic loss per capita can be observed in northwestern China and in northern  
364 parts of the northwestern China in particular.

365 At the same time, it is worth noticing that the storm related floods in the northwest  
366 region, especially in the Northwest River Basin in Xinjiang, have continued to increase  
367 during the study period. Due to the lack of rainfall stations in the northwest, it is hard  
368 to completely determine whether this phenomenon and the increase in extreme rainfall  
369 are Related, but combined with Figure 7, it can be seen that the increase in social



370 vulnerability is an important factor.

371

## 372 **5. Discussions**

373 Fig. 9 demonstrated spatial pattern of the cumulative rainfall amount and  
 374 cumulative rainfall duration of each county. Relatively complicated spatial pattern can  
 375 be identified for rainfall amount and rainfall duration. However, persistently increasing  
 376 rainfall amount and rainfall duration can be found along the northwest to southeast and  
 377 along the north to south directions. Meanwhile, Fig. 9 also clearly indicated expanding  
 378 regions with smaller rainfall amount and shortening rainfall durations. This finding  
 379 indicated amplifying droughts in northern and northwestern China with higher drought  
 380 risks but higher flood risks in southern China and southeastern China. Besides, spatial  
 381 pattern of precipitation extremes and that of flood disasters did not match well. It is  
 382 easy to understand that regions for production and confluence of runoff are often not  
 383 similar to those with occurrence of precipitation extremes (Zhang et al., 2015b). In  
 384 addition, influences of human activities and precipitation changes on streamflow are  
 385 varying for specific river basins. Damming-induced fragmentation of river basins is the  
 386 major cause behind higher homogenization of flow regimes (Zhang et al., 2015b).  
 387 Moreover, occurrence of floods do not always mean occurrence of flood disasters.  
 388 Flooding processes are mostly natural processes. However, flood disaster is closely  
 389 related to human factors such as socio-economy and population (Viero et al., 2019). All  
 390 these factors trigger spatial mismatch between floods, flood disasters, and precipitation  
 391 extremes. Furthermore, building of hydraulic infrastructure also modified spatial match



392 of floods, flood disasters and precipitation extreme (Zhang et al., 2015b).

393 Besides, the results of this study indicated increased flood frequency in both space  
394 and time. Specifically, the Yangtze River basin and Pearl River basin and the coastal  
395 regions of eastern China were dominated by higher flood frequency. However, the  
396 flood-induced death rates were decreasing in both space and time. While, remarkable  
397 increase of flood-affected people percentage and flood-induced direct loss per capita  
398 can be found in central and eastern China. Closer look is necessary on other factors  
399 besides precipitation extremes behind flood disasters and flood-induced losses in  
400 human life and economy. In this study, nine factors were selected for attribution  
401 detection based on previous researches (e.g. Hu et al., 2018), i.e. urbanization rate (the  
402 proportion of non-agricultural population in the county) (UR), population density (PD),  
403 GDP per unit area (GDPD), average elevation (ELE), river network density (RD),  
404 average slope (SLP), distance of county's geometric center from shoreline (DS), annual  
405 average heavy rainfall (VR) and annual average rainstorm duration (DR) (Fig. 10). The  
406 results were evaluated by  $q(q \in [0, 1])$  statistics, which indicated that a factor explains  
407 the  $100 \times q\%$  of the dependent variable. The larger the  $q$ , the stronger the explanatory  
408 power of an independent variable to the spatial pattern of the dependent variable. The  
409 interpretation rate of the spatial differentiation rules of the three disaster indicators of  
410 three research periods was shown in Fig. 10.

411 During 1984 and 1990, the interpretation of each factor to the affected population  
412 was relatively weak (Fig. 10a). During the period of 1991-2000, the influence of  
413 elevation, distance from the coast, heavy rainfall, and rainstorm duration on floods  
414 and/or flood disasters was significantly enhanced. With booming development of socio-



415 economy of China and fast growing population, population density and GDP per square  
416 kilometers were growing fast and all these factors gathered along the low-lying plains  
417 and along the coastal regions as well. For example, almost all megacities in China are  
418 located along the coastal regions of China such as Jing-Jin-Ji, The Yangtze Delta and  
419 the Pearl Delta regions, and these regions are highly developed with socio-economy,  
420 high-level development of science and technology. Therefore, these regions are always  
421 densely populated. Population in eastern China accounts for more than 70% of the total  
422 population of the country (Zhang et al., 2017). Therefore, these regions are usually  
423 dominated by increased flood-induced people percentage. What's more, the middle and  
424 the lower Yangtze River basin and also the Pearl River basin are often hit by flood  
425 disasters. The Yangtze Delta and the Pearl River Delta are densely populated with  
426 highly developed socio-economy. Therefore, these regions are dominated by higher  
427 flood-affected people percentage and higher flood-induced direct loss per capita.

428 Furthermore, the eastern China is characterized by low-lying terrain and this kind  
429 of topographical condition is highly sensitive to flood inundation with dense river  
430 networks. Therefore, the impact of river network density in geographical factors is also  
431 increased, indicating that the influence of low-lying terrain, high population density  
432 reflected by urbanization on rainstorm-related flood disasters is increased persistently.  
433 The main factors affecting the mortality rate were the elevation, slope, population  
434 density, GDP unit area, distance from the coast, and river network density between  
435 1984 and 2000. The geographical factors and socio-economic factors affect the spatial  
436 pattern of the flood-induced death rate. However, after 2001, the effect of above-  
437 mentioned factors on the flood-related mortality has been greatly reduced. Fig. 7 also  
438 indicated that the number of deaths due to floods has dropped significantly across the  
439 country during 1984-2007, indicating the improvement of emergency management



440 capabilities and enhanced human mitigation to flood disasters over the country. It can  
441 be seen from Fig. 10c that the main factors affecting the per capita economic loss from  
442 1991 to 2000 were urbanization rate, elevation and distance from the coast, which  
443 implied that social wealth mainly distributed in the coastal regions and/or low-lying  
444 areas. However, the effects of these influencing factors also decreased since 2001,  
445 reflecting to some extent the improvement of flood prevention and mitigation  
446 capabilities along the coast.

447

## 448 6. Conclusions

449 China is the largest country in terms of population, and is also the second economic  
450 body of the planet. Floods have been inflicting massive losses of human lives and socio-  
451 economy and higher flood risk can be expected in a warming climate. Therefore,  
452 thorough understanding flood disasters and related driving factors will be of paramount  
453 importance in both practical and theoretical sense. In this study, the spatiotemporal  
454 pattern of rainstorm-related flood disasters was analyzed with respect to trends during  
455 1984-2007. The above-mentioned results can help to achieve the following interesting  
456 and important scientific viewpoints:

457 (1) Rainfall extremes in terms of rainfall amount and rainfall duration follow no  
458 confirmative spatial pattern. Generally, increased rainstorm amount and rainstorm  
459 duration were found mainly in the lower Yangtze River basin and the middle and the  
460 lower Pearl River basin. Besides, the Huai River basin was also dominated by increased  
461 rainstorm amount and rainstorm duration. Rainstorm intensity was in complicated  
462 spatial pattern. Stations with increased rainstorm intensity distributed sporadically with  
463 stations with decreased rainstorm intensity in an exchangeable way. Besides, regions  
464 with less rainstorm amount and shorter rainstorm duration were expanding and vice



465 versa. This finding implies amplifications of floods and droughts concurrently.

466 (2) More and more counties in the central, southern, southeastern and southwestern

467 China were characterized by higher flood frequency. However, counties with high

468 flood-induced deaths decreased significantly, indicating enhanced human mitigation to

469 flood disasters. While, counties with increased flood-affected people and increased

470 direct economic loss can be identified in central and southern and southeastern China,

471 specifically the middle and lower Yangtze River basin, and the middle and the lower

472 Pearl River basin as well. It is surprising to find that some counties in the northwestern

473 China and northeastern China were also dominated by higher flood-induced mortalities,

474 which was corroborated to be the reason of a wetting tendency in the northwestern

475 China and the heavy precipitation extremes tend to occur more severely and frequently.

476 (3) There are many factors influencing spatiotemporal pattern of flood disasters and

477 relevant impacts on society. Spatial mismatch between precipitation extremes and

478 floods was attributed to many other factors. Besides, booming development of socio-

479 economy and fast growing population in China triggered fast growing population

480 density and GDP per square kilometers. Generally, the low-lying plains and coastal

481 regions are usually densely populated with high density of GDP. Therefore, these

482 regions are dominated by increased flood-induced people percentage and increased

483 direct loss of economy, and increased flood-induced direct loss per capita as well.

484 Furthermore, the eastern China is characterized by low-lying terrain and which is highly

485 sensitive to flood inundation with dense river networks. Therefore, the impact of river

486 network density in geographical factors also increased, indicating that the influence of

487 low-lying terrain, high population density reflected by urbanization on rainstorm-

488 related flood disasters increased persistently.

489





490 **Author contribution:** PH designed and carried out the experiments, and wrote the  
 491 initial version of this manuscript. QZ and CYX reviewed and improved the main text;  
 492 SS and JF helped to improve the quality of the figures.

493 **Competing interests:** The authors declare that they have no conflict of interest.

494

495 **Acknowledgments:** This work is financially supported by the National Science  
 496 Foundation for Distinguished Young Scholars of China (Grant No. 51425903), the Fund  
 497 for Creative Research Groups of National Natural Science Foundation of China (Grant  
 498 No. 41621061), National Natural Science Foundation of China (No. 41771536), the  
 499 Research Council of Norway (FRINATEK Project 274310), and by National Natural  
 500 Science Foundation of China (No. 41701103).

501

502 **Reference:**

503 Allen, M.R., Ingram, W.J.: Constraints on future changes in climate and the hydrologic  
 504 cycle. *Nature*, 419(6903), DOI:10.1038/nature01092, 2002.

505 Arnell, N.W.: Climate change and global water resources. *Global environmental change*,  
 506 9, S31-S49, 1999.

507 Cao, F., Ge, Y., Wang, J.-F.: Optimal discretization for geographical detectors-based  
 508 risk assessment. *GIScience & Remote Sensing*, 50(1), 78-92, 2013.

509 Chen, H., Sun, J.: Changes in climate extreme events in China associated with warming.  
 510 *Int J Climatol.*, 35(10), 2735-2751, 2015.

511 Cowling, A., Hall, P., Phillips, M.J.: Bootstrap confidence regions for the intensity of a  
 512 Poisson point process. *J Am Stat Assoc.*, 91(436), 1516-1524, 1996.



- 513 Daufresne, M., Lengfellner, K., Sommer, U.: Global warming benefits the small in  
514 aquatic ecosystems. *Proceedings of the National Academy of Sciences of the*  
515 *United States of America*, 106(31), 12788-12793, 2009.
- 516 Du, S., He, C., Huang, Q., Shi, P.: How did the urban land in floodplains distribute and  
517 expand in China from 1992–2015? *Environmental Research Letters*, 13(3),  
518 DOI:10.1088/1748-9326/aaac07, 2018.
- 519 Easterling, D.R., Meehl, G.A., Parmesan, C., Changnon, S.A., Karl, T.R., Mearns, L.O.:  
520 Climate extremes: observations, modeling, and impacts. *Science*, 289(5487),  
521 2068-2074, 2000.
- 522 Gaal, L., Molnar, P., Szolgay, J.: Selection of intense rainfall events based on intensity  
523 thresholds and lightning data in Switzerland. *Hydrol Earth Syst Sc.*, 18(5),  
524 1561-1573, 2014.
- 525 GLOBE Task Team, Hastings, D.A., Dunbar, P.K., Elphinstone, G.M., Bootz, M.,  
526 Murakami, H., Maruyama, H., Masaharu, H., Holland, P., Payne, J., Bryant,  
527 N.A., Logan, T.L., Muller, J.-P., Schreier, G., MacDonald, J.S.: The Global Land  
528 One-kilometer Base Elevation (GLOBE) Digital Elevation Model, Version 1.0.  
529 <http://www.ngdc.noaa.gov/mgg/topo/globe.html>, 1999.
- 530 Guha-Sapir, D., Below, R., Hoyois, P.: EM-DAT: The CRED/OFDA International  
531 Disaster Database, Université Catholique de Louvain, Brussels, Belgium.  
532 [www.emdat.be](http://www.emdat.be), 2017.
- 533 Hirabayashi, Y., Mahendran, R., Koirala, S., Konoshima, L., Yamazaki, D., Watanabe,  
534 S., Kim, H., Kanae, S.: Global flood risk under climate change. *Nature Climate*



- 535 Change, 3(9), 816-821, 2013.
- 536 Hu, P., Zhang, Q., Shi, P., Chen, B., Fang, J.: Flood-induced mortality across the globe:  
537 Spatiotemporal pattern and influencing factors. *Sci Total Environ.*, 643, 171-  
538 182, 2018.
- 539 Huang, D., Zhang, R., Huo, Z., Mao, F., Youhao, E., Zheng, W.: An assessment of  
540 multidimensional flood vulnerability at the provincial scale in China based on  
541 the DEA method. *Nat. Hazards*, 64(2), 1575-1586, 2012.
- 542 Jiang, T., Su, B., Hartmann, H.: Temporal and spatial trends of precipitation and river  
543 flow in the Yangtze River Basin, 1961–2000. *Geomorphology*, 85(3-4), 143-  
544 154, 2007.
- 545 Li, C., Cheng, X., Li, N., Du, X., Yu, Q., Kan, G.: A framework for flood risk analysis  
546 and benefit assessment of flood control measures in urban areas. *International*  
547 *journal of environmental research and public health*, 13(8), 787.  
548 DOI:10.3390/ijerph13080787, 2016a.
- 549 Li, J., Chen, Y.D., Zhang, L., Zhang, Q., Chiew, F.H.: Future changes in floods and  
550 water availability across China: Linkage with changing climate and  
551 uncertainties. *J Hydrometeorol.*, 17(4), 1295-1314, 2016b.
- 552 Li, J., Xu, N.: Classification basis and disaster reduction countermeasures of rainstorm-  
553 induced flood disasters. *Disaster Reduction In China*, 5(1), 36-39, 1995.
- 554 Li, X., Xie, Y., Wang, J., Christakos, G., Si, J., Zhao, H., Ding, Y., Li, J.: Influence of  
555 planting patterns on fluoroquinolone residues in the soil of an intensive  
556 vegetable cultivation area in northern China. *Sci Total Environ.*, 458, 63-69,



- 2013.
- Li, Y.U., Ying, X.U., Zhang, Y., Center, N.C.: Temporal and spatial variation of
- rainstorms and the impact of flood disasters due to rainstorms in China in the
- past 25 years. *Torrential Rain & Disasters*, 37(1), 67-72, 2018 (in Chinese with
- English abstract).
- Lu, R., Fu, Y.: Intensification of East Asian summer rainfall interannual variability in
- the twenty-first century simulated by 12 CMIP3 coupled models. *J Climate*,
- 23(12), 3316-3331, 2010.
- Mudelsee, M., Börngen, M., Tetzlaff, G., Grünewald, U.: No upward trends in the
- occurrence of extreme floods in central Europe. *Nature*, 425(6954), 166-169,
- 2003.
- Onozuka, D., Hagihara, A.: Extreme temperature and out-of-hospital cardiac arrest in
- Japan: A nationwide, retrospective, observational study. *Sci Total Environ.*, 575,
- 258-264, 2017.
- Shi, P.J.: Theory on disaster science and disaster dynamics. *Journal of Natural Disasters*,
- 11(3), 1-9, 2002.
- Shi, P.J., Wang, J.A., Hua, Z.J., Yan, D., Yi, G.E., Ying, W., Yang, M.C.: Integrated risk
- management of flood disaster in China: To balance flood disaster magnitude
- and vulnerability in metropolitan regions. *Journal of Natural Disasters*, 13(4),
- 1-7, 2004 (in Chinese with English abstract).
- Van Vuuren, D.P., Edmonds, J., Kainuma, M., Riahi, K., Thomson, A., Hibbard, K.,
- Hurt, G.C., Kram, T., Krey, V., Lamarque, J.-F.: The representative



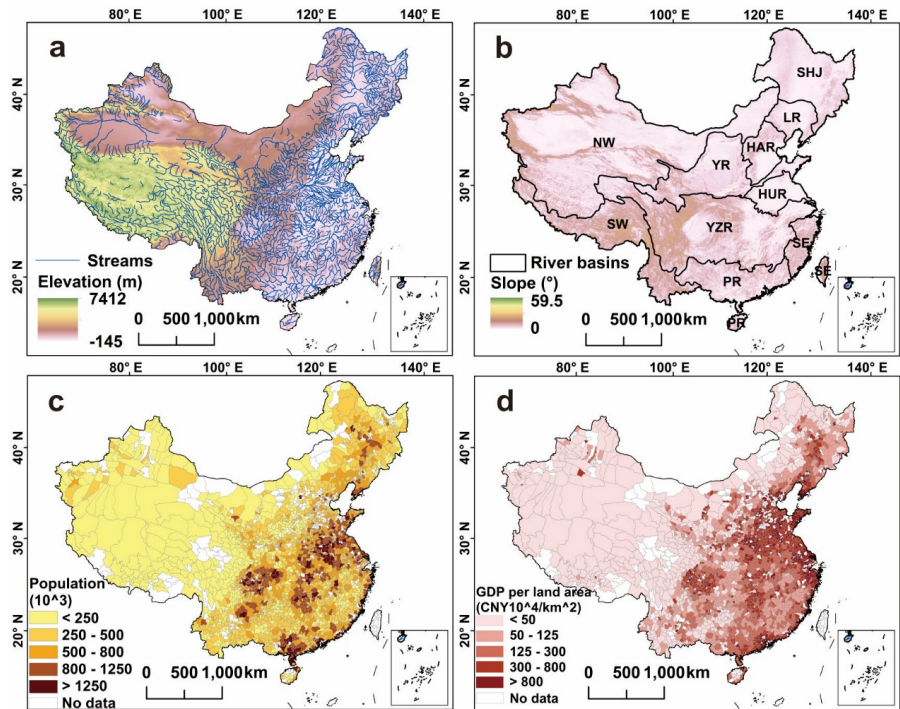
- 579 concentration pathways: an overview. *Climatic Change*, 109(1-2), 5-31, 2011.
- 580 Viero, D.P., Roder, G., Matticchio, B., Defina, A., Tarolli, P.: Floods, landscape  
581 modifications and population dynamics in anthropogenic coastal lowlands: The  
582 Polesine (northern Italy) case study. *Sci Total Environ.*, 651, 1435-1450, 2019.
- 583 Wang, J., Hu, Y.: Environmental health risk detection with GeogDetector. *Environ*  
584 *Modell Softw.*, 33, 114-115, 2012.
- 585 Wang, J., Mao, J., Jia, H.: On spatiotemporal patterns of flood and drought hazards in  
586 China. *Journal of Natural Disasters*, 1, 115-21, 2008.
- 587 Wen, K., Ding, Y.: China Meteorological Disasters Collection- China Meteorological  
588 Press. Beijing, 2008.
- 589 Wen, K., Song, L.: Collections of meteorological hazards in China- Xinjiang volume.  
590 Beijing, Meteorological Press, 2006.
- 591 Willner, S.N., Otto, C., Levermann, A.: Global economic response to river floods.  
592 *Nature Climate Change*. 8(7), 1, DOI:10.1038/s41558-018-0173-2, 2018.
- 593 Ye, J., Li, K., Kuang, S., Wang, Z.: China Flood and Drought Disaster Bulletin 2017. /  
594 Edited by The ministry of Water Resources of the People's Republic of China.  
595 China Cartographic Publishing House. Beijing, China, 2018.
- 596 Zhang, Q., Gu, X., Li, J., Shi, P., Singh, V.P.: The Impact of Tropical Cyclones on  
597 Extreme Precipitation over Coastal and Inland Areas of China and Its  
598 Association to ENSO. *J Climate*, 31(5), 1865-1880, 2018a.
- 599 Zhang, Q., Gu, X., Singh, V.P., Kong, D., Chen, X.: Spatiotemporal behavior of floods  
600 and droughts and their impacts on agriculture in China. *Global Planet Change*,



- 601 131, 63-72, 2015a.
- 602 Zhang, Q., Gu, X., Singh, V.P., Shi, P., Sun, P.: More frequent flooding? Changes in
- 603 flood frequency in the Pearl River basin, China, since 1951 and over the past
- 604 1000 years. *Hydrology & Earth System Sciences*, 22(5), 2637-2653, 2018b.
- 605 Zhang, Q., Gu, X., Singh, V.P., Sun, P., Chen, X., Kong, D.: Magnitude, frequency and
- 606 timing of floods in the Tarim River basin, China: Changes, causes and
- 607 implications. *Global Planet Change*, 139, 44-55, 2016.
- 608 Zhang, Q., Gu, X., Singh, V.P., Xu, C.Y., Kong, D., Xiao, M., Chen, X. Homogenization
- 609 of precipitation and flow regimes across China: Changing properties, causes and
- 610 implications. *J Hydrol.*, 530, 462-475, 2015b.
- 611 Zhang, Q., Li, J., Singh, V.P., Xiao, M.: Spatio-temporal relations between temperature
- 612 and precipitation regimes: implications for temperature-induced changes in the
- 613 hydrological cycle. *Global Planet Change*, 111, 57-76, 2013.
- 614 Zhang, Q., Singh, V.P., Li, J., Jiang, F., Bai, Y.: Spatio-temporal variations of
- 615 precipitation extremes in Xinjiang, China. *J Hydrol.*, 434, 7-18, 2012.
- 616 Zhang, Q., Xu, C.-Y., Zhang, Z., Chen, Y.D., Liu, C.-l., Lin, H.: Spatial and temporal
- 617 variability of precipitation maxima during 1960–2005 in the Yangtze River
- 618 basin and possible association with large-scale circulation. *J Hydrol.*, 353(3-4),
- 619 215-227, 2008.
- 620 Zhang, Q., Zheng, Y., Singh, V.P., Luo, M., Xie, Z.: Summer extreme precipitation in
- 621 eastern China: Mechanisms and impacts. *Journal of Geophysical Research:*
- 622 *Atmospheres*, 122(5), 2766-2778, 2017.



623



624

625 Fig. 1. Spatial distribution of (a) River streams (1:1,000,000) and elevation; (b) River  
626 basins (NW-Northwest river systems; SW-Southwest river systems; YR-Yellow River;  
627 YZR-Yangtze River; PR-Pearl River; SE-Southeast river systems; HUR-Huai River;  
628 HAR-Hai River; LR-Liao River; SHJ-Songhua River) and slope; (c) Population; (d)  
629 GDP per land area (2006).

630

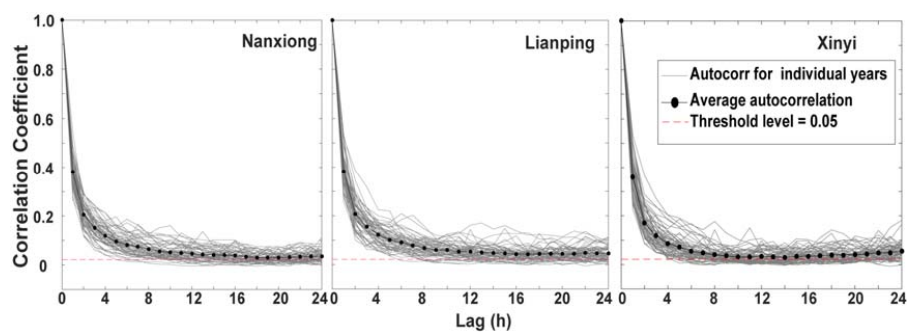
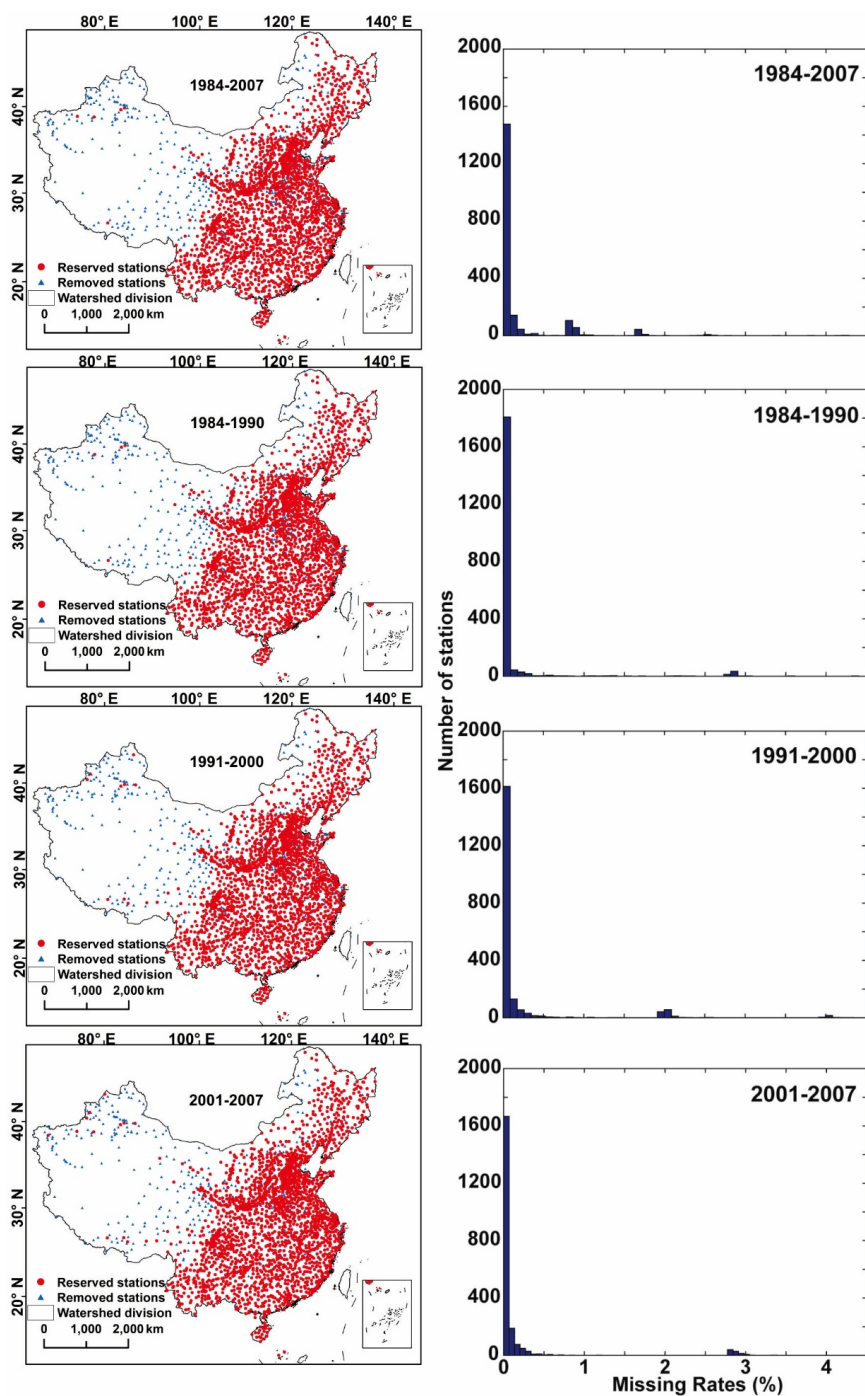


Fig. 2. Autocorrelograms for the selected three stations





634  
 635 Fig. 3. Stations screened out for analysis in this study and missing rates of the data  
 636 during different periods  
 637

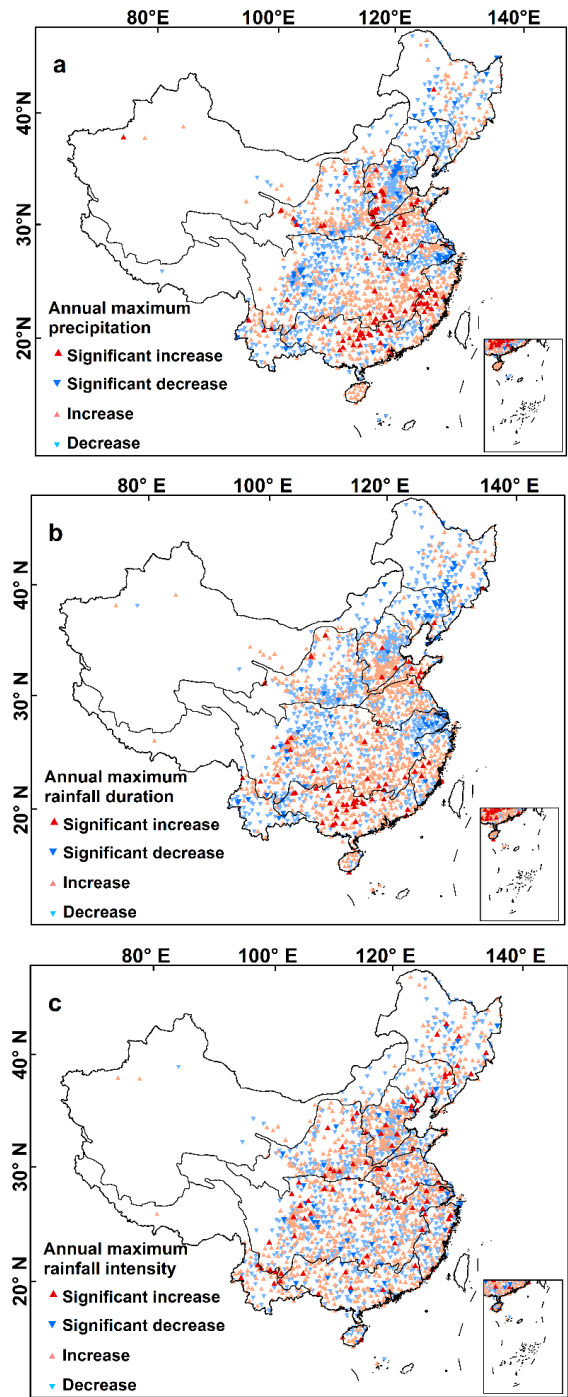


Fig. 4. Trend analysis of the maximum extreme rainfall events (a: annual maximum precipitation trend during 1984-2007; b: trend of annual maximum rainfall duration during 1984-2007; c: trend of annual maximum rainfall intensity during 1984-2007)

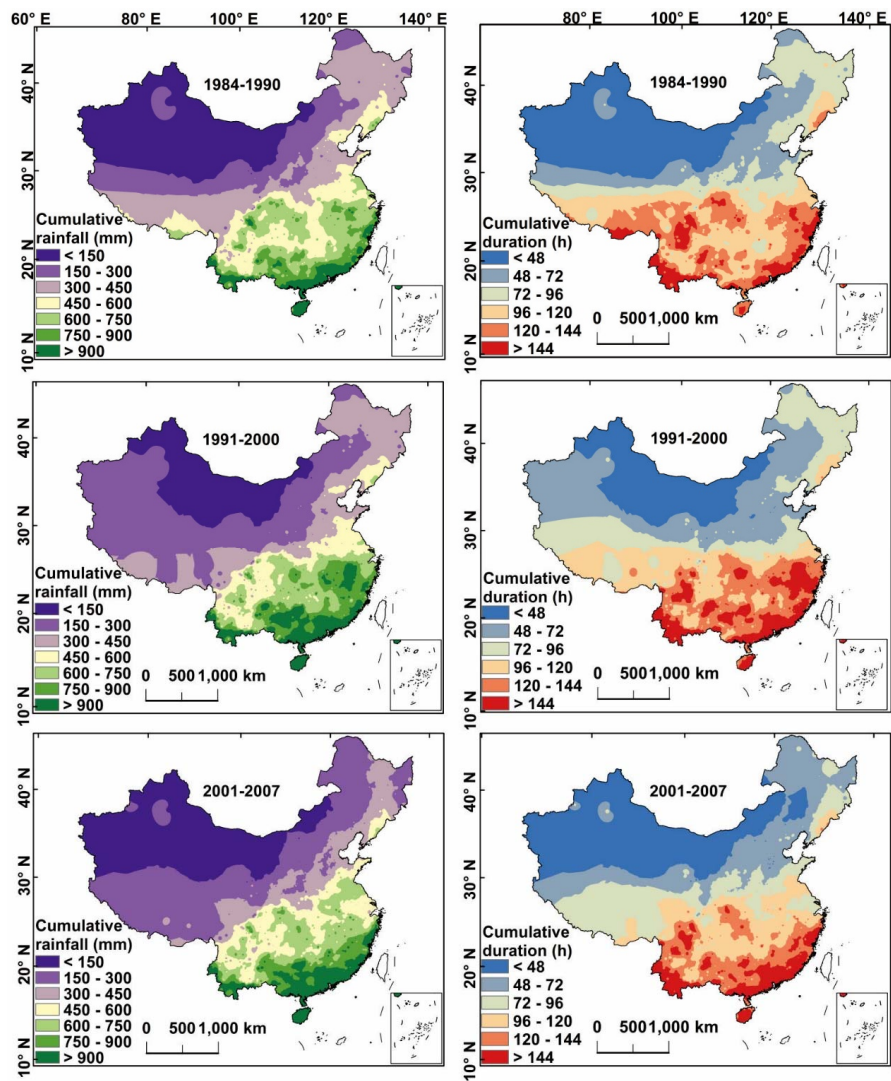


Fig. 5. Distribution of the cumulative rainfall (average annual cumulative rainfall depth of the rainstorm events) and the cumulative rainfall duration (average annual cumulative rainfall duration of the rainstorm events)

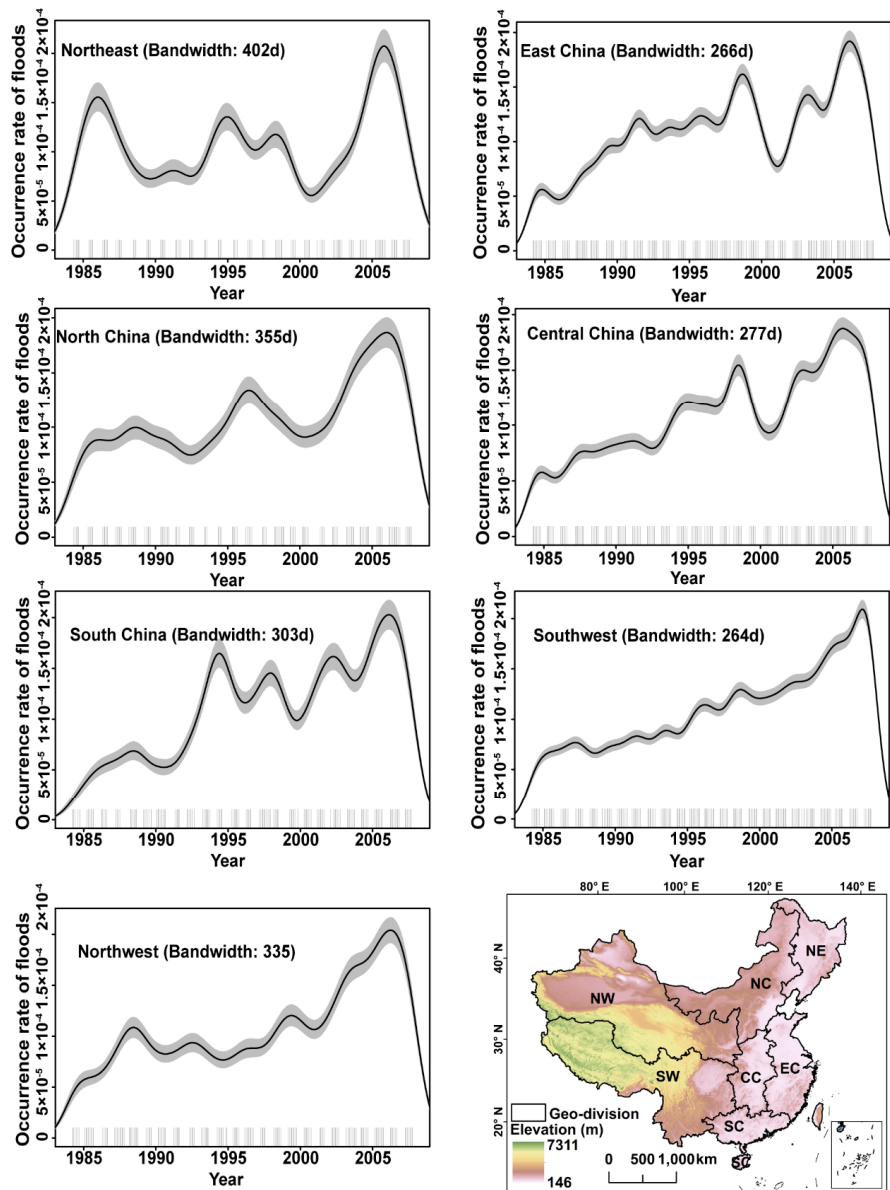


Fig. 6. Occurrence rate of flood events in seven geographical regions of China (NW-  
Northwest China; SW-Southwest China; SC-South China; CC-Centre of China; EC-  
East China; NC-North China; NE-Northeast China) in 1984-2007



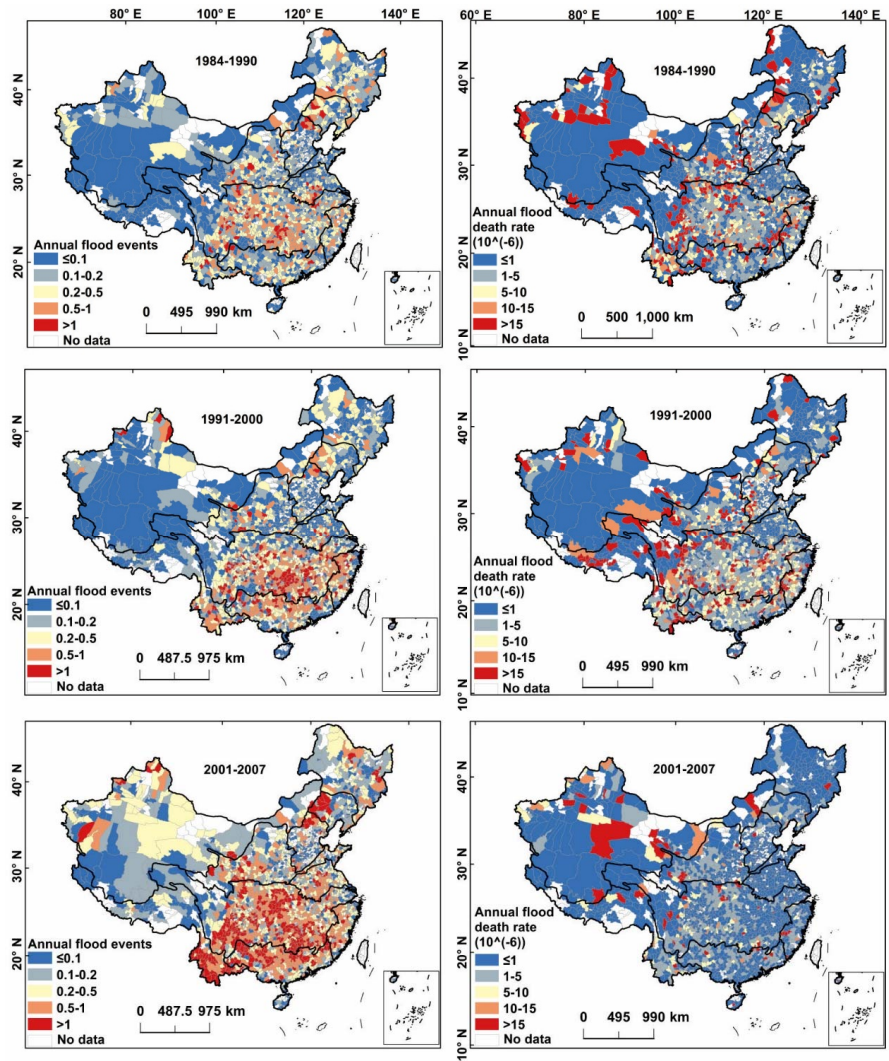


Fig. 7. Annual number of flood disasters and flood-induced death rates (ratio of flood-induced deaths to total population in each county)

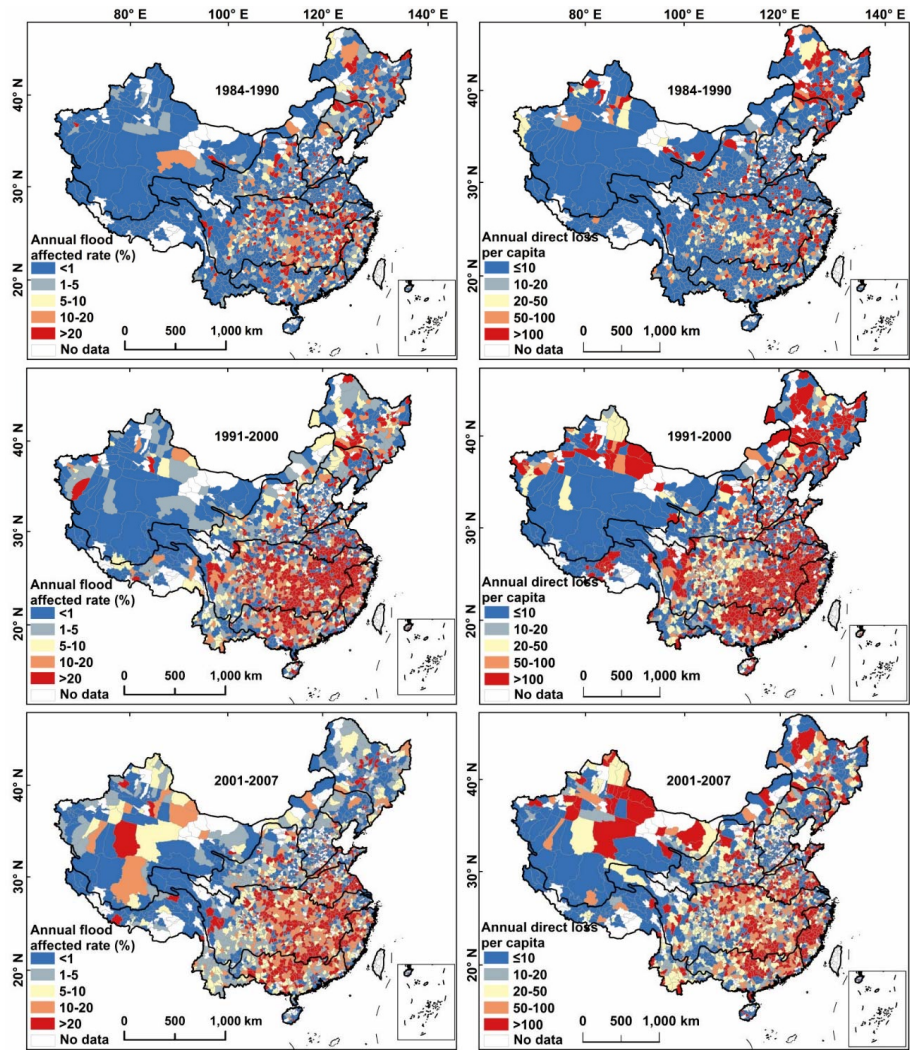


Fig. 8. Annual flood-affected rate (ratio of annual average flood affected people in the study period to total population in each county) and direct economic loss per capita (convert to the present value of 2007)

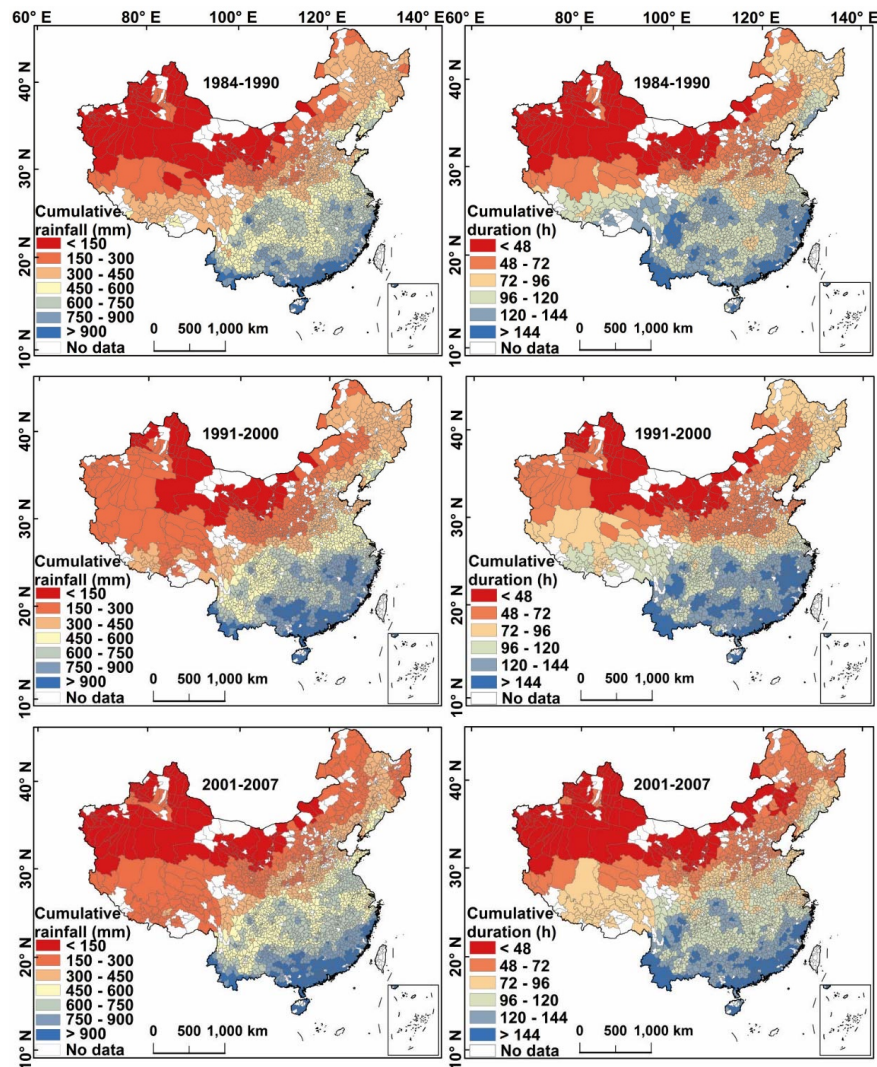


Fig. 9. Distribution of the annual cumulative intense rainfall and duration of counties (calculate average rainfall and duration of each county from results of Fig. 5)

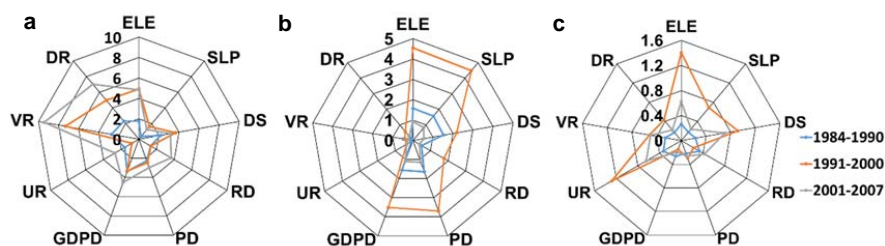


Fig. 10. Radar diagram of the contributions of meteorological and socio-economic variables (a-flood-affected people; b-flood-induced deaths; c-direct economic loss caused by flood) to the spatial distribution of flood disasters at decadal scales